The distribution of energy perturbations at planetary close encounters

Giovanni B. Valsecchi
Istituto di Astrofisica Spaziale, Area di Ricerca C.N.R.
via Fosso del Cavaliere 100, I-00133 Roma, Italy

Andrea Milani
Dipartimento di Matematica, Università di Pisa
via Buonarroti 2, I-56127 Pisa, Italy

Giovanni F. Gronchi
Dipartimento di Matematica, Università di Pisa
via Buonarroti 2, I-56127 Pisa, Italy

Steven R. Chesley
Jet Propulsion Laboratory
4800 Oak Grove Drive, CA-91109 Pasadena, U.S.A.

Abstract. Öpik's theory of close encounters allows us to deduce an analytic expression for the distribution of energy perturbations at close encounters between small bodies and planets. The derivation of this expression highlights a simple geometric structure in the plane containing the planet and perpendicular to the unperturbed planetocentric velocity vector. The analytic formulation reproduces well the results of the numerical integrations that first pointed out the asymmetries in the distribution of energy perturbations.

Keywords: perturbations, close encounters

1. Introduction

Energy perturbations at planetary close encounters undoubtedly play a major role in the transport of small bodies in the Solar System, and therefore must be correctly modelled in any study on the subject. Numerical integrations are very often used for this task. But even in numerical integrations of the equations of motion of a small body perturbed by the planets it is possible to introduce systematic errors in the computation of energy perturbations.

When the orbital evolution is dominated by close encounters it can be modelled as a stochastic process, in which case the end states are essentially determined by the asymmetries in the tails of the distribution of energy perturbations, i.e., by the difference in the frequency of occurrence between very large positive energy perturbations and very large negative ones. These asymmetries were first discovered numerically by Everhart (1969; Oikawa and Everhart 1979).

© 2000 *Kluwer Academic Publishers. Printed in the Netherlands.*

Carusi et al. (1990), Valsecchi (1992) and Valsecchi and Manara (1997) used Öpik's theory of close encounters (Öpik, 1976) to show that, in the case of small bodies on planet-crossing orbits, the distribution of energy perturbations at close planetary encounters can present significant asymmetries, depending on the semimajor axes, eccentricities, and inclinations of the orbits in question. In Valsecchi and Manara (1997) this result was confirmed by comparing the perturbation distributions obtained from numerical integrations with the results of Öpik's theory. In this paper we show that, again in the framework of Öpik's theory, it is possible to deduce an analytic expression for the distribution of energy perturbations at close encounters. The derivation of this expression allows us to highlight a simple geometric structure in the plane containing the planet and perpendicular to the unperturbed planetocentric velocity vector of the small body, the so-called b-plane.

Valsecchi and Manara (1997) remark that their use of Öpik's theory of close encounters was not intended as a fast computational tool, but as a geometric tool to explore the qualitative features of close encounter dynamics. With the increasing performances of modern computers, making the computation of a large number of close encounters less prohibitive than it used to be, the importance of Öpik's theory as a computational tool would decrease compared to its importance in the understanding of close encounter outcomes. The present paper is a further step in this same direction.

2. Energy perturbations in Öpik's theory

2.1. Geometric setup

We recall some basic formulae of Öpik's theory, following Carusi et al. (1990). The planetocentric unperturbed velocity $\vec{U}$ of a small body encountering a planet moving on a circular orbit at unit distance from the Sun (we disregard the mass of the planet in computing its heliocentric velocity) has components:

$$U_x = \pm\sqrt{2 - \frac{1}{a} - a(1-e^2)} \tag{1}$$

$$U_y = \sqrt{a(1-e^2)}\cos i - 1 \tag{2}$$

$$U_z = \pm\sqrt{a(1-e^2)}\sin i; \tag{3}$$

its absolute value is:

$$U = \sqrt{3 - \frac{1}{a} - 2\sqrt{a(1-e^2)}\cos i}. \tag{4}$$

This can be rewritten as:

$$U = \sqrt{3 - T} \tag{5}$$

where T is the Tisserand parameter with respect to the planet:

$$T = \frac{1}{a} + 2\sqrt{a(1-e^2)}\cos i. \tag{6}$$

We can introduce two angles, θ and ϕ, such that the components of $\vec{U}$ are:

$$\begin{aligned} U_x &= U \sin\theta \sin\phi && (7)\\ U_y &= U \cos\theta && (8)\\ U_z &= U \sin\theta \cos\phi && (9) \end{aligned}$$

Using the previous expressions, θ, ϕ can be obtained in terms of a, e, i:

$$\begin{aligned} \cos\theta &= \frac{\sqrt{a(1-e^2)}\cos i - 1}{\sqrt{3 - \frac{1}{a} - 2\sqrt{a(1-e^2)}\cos i}} && (10)\\ \tan\phi &= \frac{\pm\sqrt{2 - \frac{1}{a} - a(1-e^2)}}{\pm\sqrt{a(1-e^2)}\sin i}. && (11) \end{aligned}$$

Since

$$\sqrt{a(1-e^2)}\cos i = \frac{3 - \frac{1}{a} - U^2}{2}, \tag{12}$$

one can express θ, in terms of U and a, simply as:

$$\cos\theta = \frac{1 - U^2 - \frac{1}{a}}{2U}. \tag{13}$$

As a consequence of the close encounter with the planet, $\vec{U}$ is rotated into $\vec{U'}$, without changing the length (see Fig. 1). The angle between the two vectors is γ, that can be obtained in terms of U, m, the mass of the planet in units of that of the Sun, and b, the unperturbed minimum distance at encounter:

$$\begin{aligned} \cos\gamma &= \frac{b^2U^4 - m^2}{b^2U^4 + m^2} = \frac{b^2 - c^2}{b^2 + c^2} && (14)\\ \sin\gamma &= \frac{2mbU^2}{b^2U^4 + m^2} = \frac{2bc}{b^2 + c^2} && (15) \end{aligned}$$

the rightmost expressions have been simplified putting $c = m/U^2$. The vector $\vec{b}$ is the displacement from the planet of the intersection of the

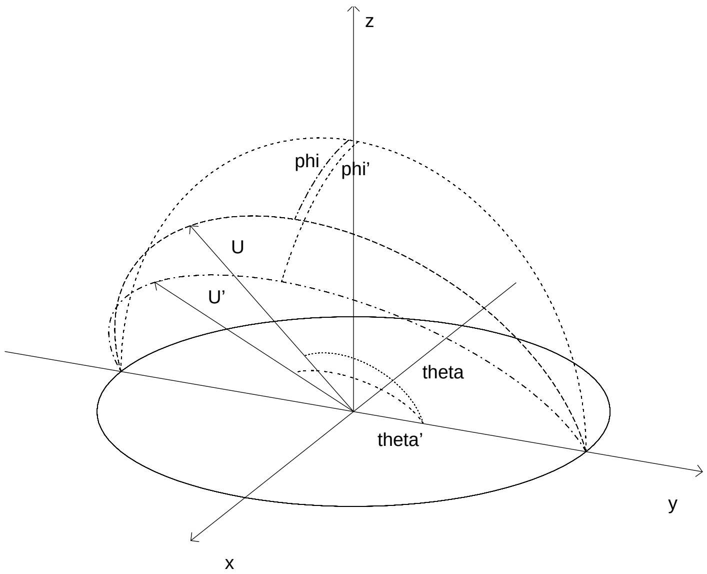

Figure 1. The geometry of the rotation of the pre-encounter planetocentric velocity vector $\vec{U}$ into the post-encounter vector $\vec{U'}$. The angle of rotation γ between $\vec{U}$ and $\vec{U'}$ is not evidenced, in order not to clutter the plot.

incoming asymptote of the planetocentric hyperbola with the b-plane, perpendicular to $\vec{U}$ and containing the planet. The b-plane is the ξ-ζ plane of a ξ-η-ζ reference frame whose η-axis is directed along $\vec{U}$, the ξ-axis is perpendicular to the heliocentric velocity of the planet, and the ζ-axis is in the direction opposite to that of the projection on the b-plane of the heliocentric velocity of the planet. We define, following Greenberg et al. (1988, Appendix, where ξ and ζ are called x and z)

$$\xi = b \sin\psi \tag{16}$$
$$\zeta = b \cos\psi, \tag{17}$$

where b is the impact parameter. The angles θ' and ϕ', defining the direction of the post-encounter velocity vector $\vec{U'}$, can be obtained in terms of θ, ϕ, γ, ψ by (Carusi et al., 1990):

$$\cos\theta' = \cos\theta\cos\gamma + \sin\theta\sin\gamma\cos\psi \tag{18}$$
$$\tan(\phi - \phi') = \frac{\sin\gamma\sin\psi}{\sin\theta\cos\gamma - \cos\theta\sin\gamma\cos\psi} \tag{19}$$
$$\tan\phi' = \frac{\tan\phi - \tan(\phi - \phi')}{1 + \tan\phi\tan(\phi - \phi')}. \tag{20}$$

U is an invariant of the problem and, once it is given, $\cos\theta$ is directly proportional to $-1/a$; the latter quantity, in turn, does not depend on

ϕ, a fact that may seem suprising. In fact, in the geometric setup just described we have fixed the heliocentric distance of the small body, thus fixing its potential energy; to obtain its total energy – that means to obtain a – we need to compute its kinetic energy, i.e. its heliocentric velocity. The latter is the vectorial sum of the heliocentric velocity of the planet, whose components are $(0,1,0)$, and of $\vec{U}$; for fixed U, this vectorial sum depends only on the angle between the two vectors, i.e. on θ.

Öpik's theory of close encounters works as long as the region of space in which the encounter takes place is "small", so that the interaction can be thought of as taking place in a point. This is not true when the Tisserand parameter approaches or even exceeds 3, i.e. when the encounters take place at low planetocentric velocity and therefore the assumption of a point-like interaction does not hold any more.

2.2. Solving for a given final semimajor axis

A given final semimajor axis a'_0 corresponds to a certain value of θ', say θ'_0:

$$\cos\theta'_0 = \frac{1 - U^2 - \frac{1}{a'_0}}{2U} \tag{21}$$

and this can be expressed by (18) as a function of θ, γ and ψ. Taking into account (14) and (15), given b we can solve for ψ:

$$\cos\psi = \frac{\cos\theta'_0 - \cos\theta\cos\gamma}{\sin\theta\sin\gamma} = \frac{(b^2+c^2)\cos\theta'_0 - (b^2-c^2)\cos\theta}{2bc\sin\theta}. \tag{22}$$

We can now compute ξ and ζ for a fixed θ'_0:

$$\xi = b\sin\psi = b\sqrt{1 - \frac{[(b^2+c^2)\cos\theta'_0 - (b^2-c^2)\cos\theta]^2}{4b^2c^2\sin^2\theta}} \tag{23}$$

$$\zeta = b\cos\psi = \frac{(b^2+c^2)\cos\theta'_0 - (b^2-c^2)\cos\theta}{2c\sin\theta}. \tag{24}$$

Solving for ξ as a function of ζ, we obtain:

$$\xi^2 = -\zeta^2 + \frac{2c\sin\theta}{\cos\theta'_0 - \cos\theta}\zeta - \frac{c^2(\cos\theta'_0 + \cos\theta)}{\cos\theta'_0 - \cos\theta}. \tag{25}$$

This is the equation of a circle centred on the ζ-axis. If R is the radius of such a circle, and D the value of the ζ-coordinate of its centre, its equation is

$$R^2 = \xi^2 + (\zeta - D)^2; \tag{26}$$

in our case, we have a circle centred in

$$D = \frac{c \sin\theta}{\cos\theta_0' - \cos\theta} \tag{27}$$

and of radius

$$|R| = \left| \frac{c \sin\theta_0'}{\cos\theta_0' - \cos\theta} \right|. \tag{28}$$

Note that $R = 0$ for $\theta_0' = 0$ and $\theta_0' = \pi$. In general, the circle intersects the ζ-axis in

$$\zeta = D \pm R = \frac{c(\sin\theta \pm \sin\theta_0')}{\cos\theta_0' - \cos\theta}, \tag{29}$$

that represent the extremal values that b can take; for $\delta\theta \to 0$ one of the two intersections goes to infinity, and the other to

$$D - R = \frac{c \cos\theta}{\sin\theta}. \tag{30}$$

The circle intersects the ξ-axis in

$$\xi = \pm c \sqrt{\frac{\cos\theta + \cos\theta_0'}{\cos\theta - \cos\theta_0'}}, \tag{31}$$

and the maximum value of $|\xi|$ for which a given θ_0' is accessible is

$$|\xi| \equiv |R| = \left| \frac{c \sin\theta_0'}{\cos\theta_0' - \cos\theta} \right|. \tag{32}$$

3. The distribution of energy perturbations

The specific heliocentric orbital energy depends only on a:

$$E = -\frac{1}{2a}, \tag{33}$$

so that, by (13), it can be seen as a function of U and $\cos\theta$ only:

$$E = \frac{U^2 + 2U\cos\theta - 1}{2}. \tag{34}$$

We have that $\cos\theta$ is then

$$\cos\theta = \frac{1 + 2E - U^2}{2U} \tag{35}$$

and $\sin\theta$ is

$$\sin\theta = \sqrt{1 - \left[\frac{1+2E-U^2}{2U}\right]^2} = \frac{\sqrt{C(E)}}{2U}, \tag{36}$$

having put

$$C(E) = -4E^2 - 4(1-U^2)E - 1 + 6U^2 - U^4. \tag{37}$$

For a given U, E behaves like a: it reaches its maximum value

$$E_{max} = \frac{U^2+2U-1}{2} \tag{38}$$

for $\theta = 0$, and its minimum

$$E_{min} = \frac{U^2-2U-1}{2} \tag{39}$$

for $\theta = \pi$. For given U and θ, i.e., for given U and E, the circles in the b-plane leading to a given E'_0 are characterized by

$$D_0 = \frac{c\sin\theta}{\cos\theta'_0 - \cos\theta} = \frac{c\sqrt{C(E)}}{2(E'_0 - E)} \tag{40}$$

$$R_0 = \frac{c\sin\theta'_0}{\cos\theta'_0 - \cos\theta} = \frac{c\sqrt{C(E'_0)}}{2(E'_0 - E)}. \tag{41}$$

Expressing the circles in terms of ξ and ζ, we have:

$$\xi^2 = -\zeta^2 + \frac{c\sqrt{C(E)}}{E'_0 - E}\zeta + \frac{c^2\left[C(E'_0) - C(E)\right]}{4(E'_0 - E)^2}. \tag{42}$$

It is clear that two circles, relative to two different values E'_1 and E'_2 of the final energy, must be contained one within the other, as they cannot intersect: if they did, the intersection points would lead to two different values of the post-encounter energy, which is clearly impossible.

Let us assume a parallel beam of small bodies, all with the same U, θ, ϕ, arriving on the b-plane with a uniform number density per unit area. The number of such bodies perturbed into orbits with energies in the interval between E'_1 and E'_2 must be proportional to the area enclosed between the two relevant circles on the b-plane:

$$\int_{E'_1}^{E'_2} f(E')dE' \propto \frac{c^2C(E'_1)}{4(E'_1 - E)^2} - \frac{c^2C(E'_2)}{4(E'_2 - E)^2}. \tag{43}$$

This expression is a valid approximation only as long as the circles do not intersect the circle centred on the planet of radius B, where B is

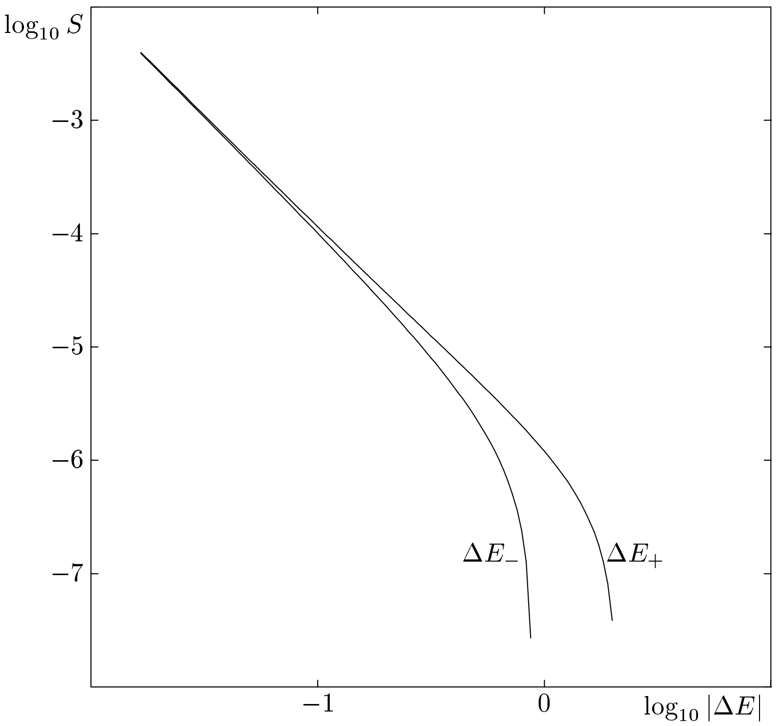

Figure 2. Log-log plot of the surface area S of the circle corresponding to a given energy perturbation, done separately for positive and negative perturbations, for a population of comets on parabolic orbits with $q = 0.52$ AU and $i = 27°$, undergoing a close encounter with Jupiter; this case is the same as that of Everhart (1969). The unit for S is the orbital radius of Jupiter to the square, and for ΔE is the specific orbital energy of Jupiter.

a suitably defined *radius of action*. Beyond B, the 2-body approximation used in Öpik's theory of close encounters becomes questionable; a typical value that is often used for B is the radius of Hill's sphere:

$$B = \sqrt[3]{\frac{m}{3}}, \tag{44}$$

although other choices are possible.

As said before, Everhart (1969, Fig. 1) discovered that the tails of the distribution of energy perturbations are in general asymmetric; Everhart studied the encounters with Jupiter of an ensemble of comets on parabolic orbits, all with $q = 0.52$ AU and $i = 27°$. These comets have all the same value of U, and we have therefore used this value to compute the surface area S of the circle corresponding to a certain post-encounter energy E'. The results are plotted in Fig. 2, and are limited to circles completely contained within the distance B, defined by (44), from Jupiter; the circles not taken into account are anyway

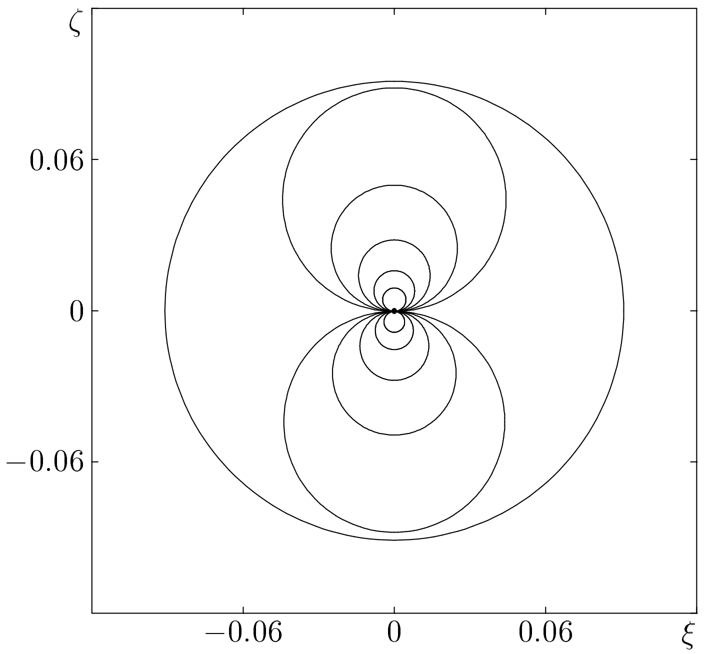

Figure 3. The b-plane circles for the comets of Fig. 2. The position of Jupiter is marked with a dot, and the radius of the outer circle centred on the planet is given by (44); the unit of length is the orbital radius of Jupiter. The five circles in the upper part of the plot correspond to positive energy perturbations of, from the largest circle to the smallest, $\log_{10} \Delta E = -1.75, -1.5, -1.25, -1, -0.75$, while those in the lower part correspond to negative energy perturbations of, again from the largest circle to the smallest, $\log_{10} |\Delta E| = -1.75, -1.5, -1.25, -1, -0.75$. Note how radii of the smaller circles in the upper part of the Figure are slightly larger than the radii of the corresponding circles in the lower part.

not of interest here, because they correspond to distant perturbations, for which the asymmetry is not present.

The Figure reproduces well the results by Everhart, thus showing the validity of our analytic expressions. Note that also Carusi et al. (1990) showed that Öpik's theory allows us to reproduce Everhart's result (see their Fig. 9); what is different in the present treatment is the analytic expression for the locus of points on the b-plane leading to the same energy perturbation, and the understanding of its geometry.

The latter is shown in Fig. 3, where the b-plane of Everhart's comets is plotted, together with the circle of radius given by (44) and a number of circles corresponding to different energy perturbations. The slower decrease in radius of the circles corresponding to positive energy perturbations (those in the upper part of the Figure) is noticeable.

4. Conclusions

For a small body undergoing a close encounter with a planet, the initial conditions leading to a post-encounter orbit of given semimajor axis share a simple geometric property: in the b-plane (containing the planet and perpendicular to the unperturbed planetocentric velocity) these initial conditions lay on a circle; the radius of this circle is a simple function of the planetocentric velocity, and of the pre- and post-encounter orbital energies. Moreover, the centre lays on the projection on the b-plane of the heliocentric velocity of the planet, at a distance from it that is again a simple function of the planetocentric velocity, and of the pre- and post-encounter orbital energies. Starting from these analytical functions, it is possible to derive a simple analytic expression for the distribution of energy perturbations at close encounters that correctly reproduces the well known asymmetries of their tails.

References

Carusi, A., G.B. Valsecchi, and R. Greenberg. Planetary close encounters: geometry of approach and post-encounter orbital parameters. *Celest. Mech. & Dynam. Astron.* 49: 111–131, 1990.

Everhart, E. Close encounters of comets and planets. *Astron. J.* 74: 735–750, 1969.

Greenberg, R., A. Carusi, and G.B. Valsecchi. Outcomes of planetary close encounters: a systematic comparison of methodologies. *Icarus* 75: 1–29, 1988.

Oikawa, S., and E. Everhart. Past and future orbit of 1977 UB, object Chiron. *Astron. J.* 84: 134–139, 1979.

Öpik, E.J. *Interplanetary Encounters.* Elsevier, New York, 1976.

Valsecchi, G.B. Close encounters, planetary masses and the evolution of cometary orbits In J.A. Fernández and H. Rickman, editors, *Periodic Comets*, pages 81-96. Universidad de la República, Montevideo, 1992.

Valsecchi, G.B. and A. Manara. Dynamics of comets in the outer planetary region. II Enhanced planetary masses and orbital evolutionary paths. *Astronomy and Astrophysics* 323: 986–998, 1997.